

PRANAS: A new platform for retinal analysis and simulation

Bruno Cessac, Pierre Kornprobst, Selim Kraria, Hassan Nasser, Daniela Pamplona, Geoffrey Portelli, Thierry Viéville

► To cite this version:

Bruno Cessac, Pierre Kornprobst, Selim Kraria, Hassan Nasser, Daniela Pamplona, et al.. PRANAS: A new platform for retinal analysis and simulation. [Research Report] RR-8958, Inria Sophia Antipolis; Inria Bordeaux Sud-Ouest. 2017, pp.27. hal-01377307v2

HAL Id: hal-01377307

<https://hal.inria.fr/hal-01377307v2>

Submitted on 24 Aug 2017

HAL is a multi-disciplinary open access archive for the deposit and dissemination of scientific research documents, whether they are published or not. The documents may come from teaching and research institutions in France or abroad, or from public or private research centers.

L'archive ouverte pluridisciplinaire **HAL**, est destinée au dépôt et à la diffusion de documents scientifiques de niveau recherche, publiés ou non, émanant des établissements d'enseignement et de recherche français ou étrangers, des laboratoires publics ou privés.



PRANAS: A new platform for retinal analysis and simulation

B. Cessac, P. Kornprobst, S. Kraria, H. Nasser, D. Pamplona, G. Portelli, T. Viéville

The authors are listed in alphabetical order

**RESEARCH
REPORT**

N° 8958

August 2017

Project-Teams Biovision and
Mnemosyne



PRANAS: A new platform for retinal analysis and simulation

B. Cessac*, P. Kornprobst*, S. Kraria*, H. Nasser*, D. Pamplona*, G. Portelli*, T. Viéville†

The authors are listed in alphabetical order

Project-Teams Biovision and Mnemosyne

Research Report n° 8958 — August 2017 — 24 pages

Abstract: The retina encodes visual scenes by trains of action potentials that are sent to the brain via the optic nerve. In this paper we describe a new free access user-end software allowing to better understand this coding. It is called PRANAS (<https://pranas.inria.fr>), standing for Platform for Retinal ANalysis And Simulation. PRANAS targets neuroscientists and modelers by providing a unique set of retina-related tools. PRANAS integrates a retina simulator allowing large scale simulations while keeping a strong biological plausibility and a toolbox for the analysis of spike train population statistics. The statistical method (entropy maximization under constraints) takes into account both spatial and temporal correlations as constraints, allowing to analyze the effects of memory on statistics. PRANAS also integrates a tool computing and representing in 3D (time-space) receptive fields. All these tools are accessible through a friendly graphical user interface. The most CPU-costly of them have been implemented to run in parallel.

Key-words: Retina simulator, spike train statistics, population coding, maximum entropy, Gibbs distributions, large scale spiking activity, spike train generation, multi-electrode array recordings

* Université Côte d’Azur, Inria, Biovision team, France

† Inria, Mnemosyne project team, Bordeaux, France

**RESEARCH CENTRE
SOPHIA ANTIPOLIS – MÉDITERRANÉE**

2004 route des Lucioles - BP 93
06902 Sophia Antipolis Cedex

PRANAS: Une nouvelle plateforme pour l'analyse et la simulation de rétines

Résumé : La rétine encode les scènes visuelles par des trains de potentiels d'action qui sont envoyés au cerveau via le nerf optique. Dans cet article, nous décrivons un nouveau logiciel libre d'accès qui permet de mieux comprendre ce codage. Il s'appelle PRANAS (<https://pranas.inria.fr>), ayant pour signification *Platform for Retinal ANalysis And Simulation*. PRANAS cible les neuroscientifiques et les modélisateurs en fournissant un ensemble unique d'outils liés à la rétine. PRANAS intègre un simulateur de rétine permettant des simulations à grande échelle tout en conservant une forte plausibilité biologique et une boîte à outils pour l'analyse statistique des trains d'impulsion dans une population de neurones. La méthode statistique (maximisation de l'entropie sous contraintes) prend en compte les corrélations spatio-temporelles comme contraintes, permettant d'analyser les effets de la mémoire sur les statistiques. PRANAS intègre également un outil de calcul et de représentation en 3D (temps-espace) des champs récepteurs. Tous ces outils sont accessibles grâce à une interface utilisateur conviviale. Les plus coûteux d'entre eux en terme de temps de calculs ont été implémentés pour fonctionner en parallèle.

Mots-clés : Retina simulator, spike train statistics, population coding, maximum entropy, Gibbs distributions, large scale spiking activity, spike train generation, multi-electrode array recordings

1 Introduction

The retina is one of the most developed sensing devices [21, 34, 35]. It transforms the incoming light into a set of electrical impulses, called spikes, which are sent asynchronously to higher level structures in the visual cortex through the optic nerve. Although Cajal’s neuron doctrine was postulated more than one century ago, how information is encoded and transmitted by neurons is still not entirely understood today. Especially, the role of spatio-temporal correlations in population coding raises up deep theoretical and practical questions that are far from being answered [49, 6], particularly for the visual information transmitted from the retina to the visual cortex. To address these questions and make progress in their understanding, one needs to develop joint modeling and experimental studies with efficient software to analyse data. In this paper we present a new Platform for Retinal ANalysis And Simulation called PRANAS (<https://pranas.inria.fr>). It was designed as a user-friendly tool dedicated to neuroscientist community in a large sense, i.e., not only experienced computational neuroscientists. It has two main goals, analyse retina data, especially spatio-temporal correlations, and simulate the spike response of the retina to a visual flow. This makes this tool a unique platform to better understand how the retina works.

The first goal of PRANAS is to provide methods to analyse retinal recordings at single cell and population levels. With the advent of new techniques, the recording of the simultaneous activity of groups of neurons provides a critical database to unravel the role of specific neural assemblies in spike coding. The acquisition capacity of Multi-Electrode Arrays (MEA) has been exponentially increasing over years [57]. Systems like the 256-MEA has become a standard although new high-density MEA are now available such as the APS CMOS 4096-electrodes [15]. Using these systems, one can record from hundreds to thousands of neurons simultaneously in the retina (and more generally in vivo or in vitro, from cultures of neurons, and from other brain areas). As one gains more intuitions and results on the importance of concerted activity in spike trains, models are developed to extract, from animal recordings, possible canonical principles underlying spike coding. This is a major challenge with many potential outcomes. Beyond the dream that population coding is ruled by a few first principles, several applications could emerge such as the development of artificial systems having similar levels of performance as biological systems. To this end, accurate tools are required to analyse and compare spike trains, experimental or computer generated ones. Progress has been made recently to analyse spike trains [53, 54, 32, 62, 61, 52, 51, 50]. Especially, the spatio-temporal aspects (memory) and causality have been shown to be relevant for exploring neural activity [6]. For instance, [68] and [60] demonstrated the importance of temporal statistics and [42, 40] developed new tools to analyse spatio-temporal activity for large scale spiking networks. These methods shed a new light on spike train analysis. However, they require time and expertise to be implemented efficiently, making them hard to use. The idea of developing a new software came from our motivation to share these recent developments with the neuroscience community in a broad sense. PRANAS integrates all our expertise in terms of spike trains statistical analysis. Note that other methods analyzing correlations in massively parallel data using completely different approaches have also been proposed [26, 59, 65, 47].

The second goal of PRANAS is to provide a customizable retina simulator which could evolve in synergy with experimental data analysis. Currently, there is a large and expanding body of literature concerning models of retinal processing. There are three main classes of models. The first class regroups the linear-nonlinear-poisson (LNP) models [43]. LNP models can simulate the spiking activity of ganglion cells (and of cortical cells) in response to synthetic or natural images [3] but they voluntarily ignore the neuronal mechanisms and the details of the inner retinal layers that transform the image into a continuous input to the ganglion cell (or any

type of cell) stages. The second class of models has been developed to serve as a front-end for subsequent computer vision task. They provide bio-inspired modules for low level image processing. One interesting example is given by [2, 23], where the model includes parvocellular and magnocellular pathways using different non-separable spatio-temporal filter that are optimal for form- or motion-detection. The third class is based on detailed retinal models reproducing its circuitry, in order to predict the individual or collective responses measured at the ganglion cells level [44, 69, 31, 33]. In PRANAS, we are interested in this third class of models because they allow to explore several aspects of retinal image processing such as (i) understanding how to reproduce accurately the statistics of the spiking activity at the population level [41], (ii) reconciling connectomics and simple computational rules for visual motion detection [29] and (iii) investigating how such canonical microcircuits can implement the different retinal processing modules cited in, e.g., [21]. More precisely, the PRANAS platform has integrated and extended the VIRTUAL RETINA simulator [69]¹ initially developed in our team to do large scale retina simulations. VIRTUAL RETINA has been used in several theoretical studies [37, 39, 1, 11, 12, 66].

This paper, aiming at presenting this new platform PRANAS, is organized as follows. In Sec. 2, we give an overview of PRANAS and compare it with a selection of other tools currently available focusing on spike train analysis methods. In Sec. 3, we present the main features of the software. Illustrations and step by step procedures are given in several cases allowing readers to reproduce them. In Sec. 4, we discuss future developments.

2 General presentation

PRANAS targets a broad community of scientists interested in exploring spike coding, in particular at retina level. It provides new tools for analyzing spike trains at the population level and several methods to generate them, either with a prescribed statistics (including spatio-temporal correlations) or by emulating the retinal response to a visual scene. This is done through a user-friendly Graphical User Interface (GUI). PRANAS runs on multiple platforms (Linux, Mac OS, Windows) and it supports parallel architectures. The software is provided as binary code or as source code on request upon acceptance on the terms of the license given on the website (<http://pranas.inria.fr>). Documentation, tutorials, and samples of spike trains are also available.

The GUI of PRANAS (version 1.0.0) has three main panels, as shown in Fig. 1:

- Function panel (**FP**) is the main panel containing Input/Output interfaces and functions. It is organized in three sections: **Data**, **Analysis** and **Simulation**. (see Sec. 3 for more details).
- The parameter panel (**PP**) allows one to set parameters related to the chosen function from the function panel.
- The results panel (**RP**) contains the results. Several results can be displayed simultaneously in different subpanels, and each result can be exported as a figure in a variety of formats (e.g., PDF, PNG, JPG). The user can change the **Number of views** and which result should be displayed in each subpanel. In most subpanels, there are icons on the left-hand side to open, save, export or change plot settings (see Fig. 1(c)). Another example is shown in Fig. 4(a) (**Stimulus view**) where the user can export, show/hide grid and spikes and select neurons graphically.

¹VIRTUAL RETINA website: <http://virtualretina.inria.fr>

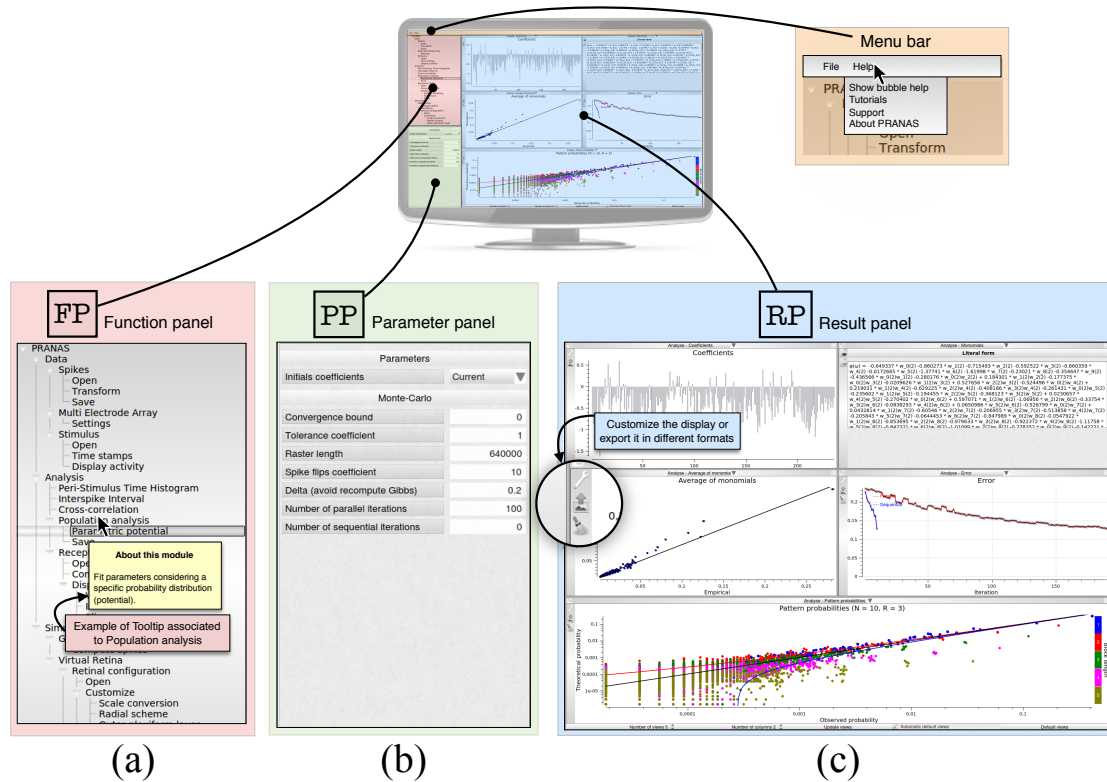


Figure 1: Presentation of PRANAS GUI panels. (a) Function panel (**FP**) is the main panel containing Input/Output interfaces and functions. It is organized in three sections: **Data**, **Analysis** and **Simulation**. Note that in the **Help** option from the menu bar users can select **Show bubble help** which will trigger tooltips giving information for each function. (b) Depending on the function selected, the parameter panel (**PP**) gives the opportunity to set the corresponding parameters. (c) Results panel (**RP**) can show all results the user want. The number of sub-panels and the windows to show can be changed. Note that for each result shown in a sub-panel, the user can customize the display or export it in different formats.

Finally, another convenient feature of the software is that user can save what he has done in term of analysis in a HDF5 file [70] (**File>Save**) and load it later to continue the work.

PRANAS is implemented in C++. It has its own dedicated libraries. It also uses other libraries for storage (HDF5), analysis (GSL, SFMT), display and GUI (Qt4, Qwt, VTK, CImg). Some parts of the software, especially the statistical estimations, run on multiple processors thanks to OpenMP framework. The software takes all the available processors in the machine automatically, without any interaction with the user. Parallelization allows to boost heavy computations and save processing time and memory.

To our best knowledge there is no other platform integrating together the functionalities proposed by PRANAS, to both analyse and stimulate retinal activities. There are however several platforms performing efficient spike train analysis. Table 1 provides a qualitative comparison between PRANAS and a selection of such tools for spike train analysis. We note that the implementation of PRANAS as a stand-alone application in C++/Qt4 rather than a library (such as, e.g., the FIND toolbox) makes this tool readily available without the need of an external in-

terpreter, such as Python or the commercially available Matlab suite (MathWorks, Natick, VA). Thus, access to PRANAS functions from a scripted analysis is performed via command line calls (see Sec. 4).

	CX	FD	NT	SL	NY	OY	ET	SR	NE	SV	PS
Version	2.12	2.0	2.0	1.00	0.1	0.3.5	0.3.0	0.3-2	5.037	0.4.2	1.0.0
Language	Matlab	Matlab	Matlab	Matlab	Python	Python	Python	R	VB	Python	C++
GUI	●	●		●		●			●	●	●
Scripting	●	●	●	●	●	●	●	●	●	●	
Free binary	●	●	●	●	●	●	●	●		●	●
File formats (Nex)		●		●	●	●	●		●	●	●
File formats (HDF5)		●				●	●			●	●
Rate histogram PSTH				●	●		●		●	●	●
Population PSTH	●	●		●	●		●		●	●	●
ISI	●	●		●	●		●	●	●	●	●
Cross-correlograms	●	●		●	●		●	●	●	●	●
Joint spike and stimulus visu.											●
STA					●	●	●		●		●
PCA									●		
Spectral analysis	●				●	●	●		●	●	
MaxtEnt (x / x-t)			GLM								●
Raster generation					●		●				●
... with Poisson / Non Poisson					●		●				●
... with VIRTUAL RETINA											●

Table 1: Comparison between a selection of existing software for spike train analysis. Abbreviations for software names (first and last initials) have been chosen for the presentation. Following software is discussed: **CX**: CHRONUX [27], **FD**: FIND [38], **NT**: NSTAT [20], **SL**: SIGTOOL [30], **NY**: NEUROPY [56], **OY**: OPENELECTROPHY [18], **ET**: ELEPHANT, **SR**: STAR [45], **NE**: NEUROEXPLORER, **SV**: SPYKEVIEWER [46], and **PS**: PRANAS. Note that features selected in this table have essentially been chosen according to what PRANAS does. It is not an exhaustive list and information applies to the time of writing. Software we mention can have additional features not commented herein.

3 PRANAS main functions

3.1 Data

In section **Data**, user can load spike trains files. Spikes may come either from real cells recordings or from a simulated spiking neural network. They can be imported from different formats such as simple text file (**.txt**), DAT file for Windows (**.dat**), NEXUS file (**.nex**) or HDF5 file format (**.hdf5**, see [70]) allowing to store not only the spikes but also other information related to experimental protocole (e.g., time stamps, MEA characteristics).

Depending on how the spikes were generated, the user can also load other information such as:

- The MEA configuration for animal cell recordings, allowing the spiking activity to be displayed relative to the grid of electrode.

- The sequence of images in case of a visual experiment, allowing the spiking activity to be displayed together with the stimulus but also to emulate a retinal response (see Sec. 3.3.2).
- The image time stamps, i.e., the precise time at which each image was shown, allowing to perform Spike-Triggered-Average (STA) [8].

3.2 Analysis

3.2.1 Classical analysis

Once the spikes are available (simulated or imported), different analysis can be performed starting with basic visualizations and classical analysis such as peri-stimulus histogram, interspike interval, and cross-correlation (see Fig. 2 and Example 1). The number of neurons used for the analysis can be of several thousands, although the user can select subsets of neurons according to different criteria, e.g., individual activity or receptive field localization (if applicable, i.e., if data allows to compute receptive fields). Even for a large population of neurons (about 4000 neurons), on any modern computer, the computational time of most of the functions in the classical analysis is neglectable.

Example 1 How to obtain the peri-stimulus time histogram (PSTH) on a selection of neurons having the highest spike rates?

1. **FP** `Data>Spikes>Open`
2. **PP** Browse and select the file of spikes.
3. **RP** (Optional) In the sub-panel showing the list of neurons, click on **Spike rate** to sort neurons with respect to their averaged spike rate, select the set of neurons with higher spike rate and click on **Keep selected**.
4. **FP** `Analysis>Peri-stimulus time histogram`.
5. **PP** Choose the **bin size** (time step) in milliseconds and click on **Compute**.

3.2.2 Population analysis

With the current evolution of Multi-Electrode Array (MEA) recordings devices, it is possible to record simultaneously thousands of neurons [15]. This opens up the possibility of analysing the collective neuronal population activity, namely its spatio-temporal correlations. Characterizing spatio-temporal statistics is a fundamental step toward extracting general population coding principles in neuronal networks. For example, it has been observed in several vertebrate species that, even if the pairwise correlations of retinal ganglion cell are weak, they are necessary to explain the statistics of spikes [19, 22, 53, 54, 62].

Analysing spatio-temporal correlations is, however, a notoriously hard problem from a statistical perspective. The point is not only to measure pairwise or higher order correlations but also to address adequately the question of their significance in neuronal coding taking into account constraints such as limited statistical sample, the reliability of statistical tests, the hypotheses underlying mathematical models and risks of overfitting [51, 52]. One possible way of solving this problem is to use Gibbs distributions. Initially introduced in statistical physics by Boltzmann and Gibbs [28] but currently used in a broader context, this general class of probability distributions, constitutes a canonical paradigm to explain the spike statistics reproducing as close as possible empirical correlations, without adding additional unnecessary assumptions [53, 54, 32, 61, 16, 17, 62, 61]. This method has been used to study pairwise correlations (see [68, 42, 40] as well as more general spatio-temporal correlations [7, 67, 9, 42, 10, 24, 48, 25].

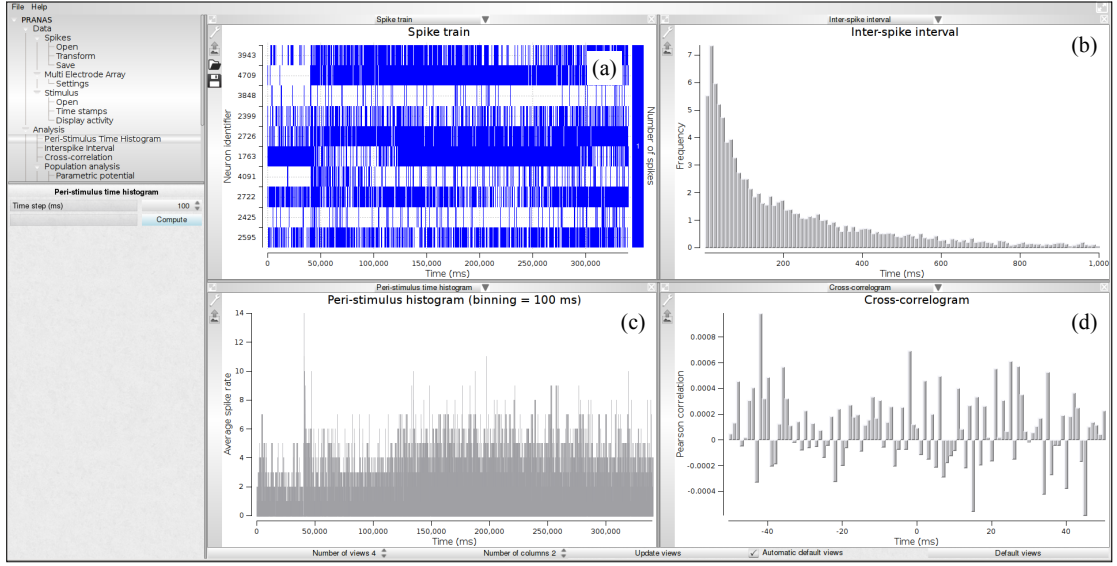


Figure 2: Example of classical analysis for a spike train shown in sub-panel (a). The following estimations are shown: (b) Inter-spike interval (ISI), (c) Peri-stimulus time histogram (PSTH) and (d) cross-correlogram. Data from electrode array recording of a mouse retina in response to a moving pattern.

PRANAS provides a toolbox to compute a Gibbs distribution from the neuronal data *i.e.*, to estimate a probability distribution, reproducing as close as possible empirical space- and time-statistics of a raster, without adding additional unnecessary assumptions (maximizing entropy)². In the current version, the population analysis toolbox of PRANAS focuses on stationary distributions, *i.e.*, the statistics are invariant under time-translation. We give first a brief explanation of Gibbs distribution before explaining how to use PRANAS (see [67, 42, 40] for more details).

Below, rasters are denoted by ω . We assume that time has been discretized with some time bin. The state of neuron i at time t is denoted by $\omega_i(t) \in \{0, 1\}$. We note by $\omega(t)$ the vector $\omega_i(t)$ (it tells us the spiking state of neurons at time t). Therefore, a raster ω is mathematically a matrix with N lines (number of neurons) and T columns (time bins in the raster). Obviously, it is not stored this way in memory (we do not store 0s). A Gibbs distribution is a probability measure μ defined by a function E (also called "energy"). The probability of observing a raster ω of time length T , $\mu[\omega]$ is proportional to $e^{E(\omega)}$ where $E(\omega) = \sum_{t=1}^T \phi(\omega(t))$. In the following ϕ is called "potential". A paradigmatic example of Gibbs distribution appears in the Ising³ model. Here $\phi(\omega(t)) = \sum_i b_i \omega_i(t) + \sum_{i,j} J_{ij} \omega_i(t) \omega_j(t)$ where the sums hold on neurons indices. The terms b_i, J_{ij} are parameters tuning the probability whereas the terms $\omega_i(t), \omega_i(t) \omega_j(t)$ depend on the spike configuration and are called "interactions" (self-interaction for the term $\omega_i(t)$, and

²Note that this toolbox first motivated the creation of the GUI to manipulate these complex notions. In former publications, software was named ENAS standing for Event Neural Assembly Simulations. After fusing of ENAS and the retina simulator VIRTUAL RETINA (see Sec. 3.3.2) into the same platform, we decided to choose a better suited name (PRANAS) to describe the functional scope of this unique platform allowing to (i) analyse spike trains coming from simulations or MEA recordings, at single cells or population levels, (ii) simulate retinal spike trains from a bio-plausible model, (iii) use additional dedicated tools for retinal recordings.

³The model initially proposed by Ising and Lenz in 1920 had only nearest neighbours interactions and constant couplings. The potential form we use corresponds in fact to a spin-glass but we use here the terminology found in computational neuroscience papers.

pairwise interactions $\omega_i(t)\omega_j(t)$. Here parameters b_i, J_{ij} are independent on time (stationarity assumption) so it is sufficient to define the potential ϕ at time $t = 0$.

In the Ising model, there is no coupling of spikes at different times so that the probability of observing a raster of length T factorizes into probabilities of spike states $\omega(t)$: consecutive time events are therefore independent. We say the statistical model has "no memory" in contrast to the Markovian model presented now. A natural generalization of the Ising form is indeed to define the potential ϕ as:

$$\phi(\omega) = \sum_{l=0}^L h_l m_l(\omega) \quad (1)$$

The terms h_l are parameters tuning the probability. They correspond to b_i, J_{ij} in Ising model but they tune more general spike interactions. Again, these parameters are independent of time (stationarity) so that we can define the potential ϕ starting from an initial time 0. The main difference with Ising model is that now interactions involve spikes at different times t_1, \dots, t_n . These interactions correspond to the terms $m_l(\omega)$, with the general form $\omega_{i_1}(t_1) \dots \omega_{i_n}(t_n)$, i.e. it involves spike events occurring at different times. As an immediate consequence, consecutive time events are not independent anymore. One can show the Gibbs distribution is, in this case, the invariant probability of a Markov chain. Thus, statistics involves memory and has nonvanishing time correlations. For historical reasons, related to the development of our research work, we call from now the m_l s "monomials" instead of "interactions". The monomials correspond thus to the conjunction of events in the raster, varying the space and time. For instance, the condition "neuron zero is firing at time one, neuron two is firing at time zero and neuron three is firing at time two" corresponds to $m(\omega) = \omega_0(1)\omega_2(0)\omega_3(2)$. More generally, the times t_k defining a monomial are chosen in the interval $[0, D]$ where D is a positive integer characterizing the memory depth of the Markov chain associated with the Gibbs distribution. The model range is given by $R = D + 1$. The potential range is directly connected to the complexity of the algorithm analyzing data, as the higher the range the higher the computational time and memory load. Gibbs distributions satisfy a variational principle: maximizing the statistical entropy under the constraints that the average value of each monomial, $\mu[m_l]$ has a fixed value. Gibbs distributions are thus also called Maximum Entropy (MaxEnt) distributions. In our case, this value is equal to average empirical value $\pi[m_l]$ computed from an experimental raster. In other words, here is what our algorithm does: given an initial form of the potential ϕ , fixed by the user (see below), one seeks the parameters h_l maximizing the statistical entropy under the constraints $\mu[m_l] = \pi[m_l]$. In general, it is not possible to have the strict equality $\mu[m_l] = \pi[m_l]$ so one tries to approach it at best. Equivalently, we minimize the Kullback-Leibler divergence between μ , the "model" and π the empirical measure ("data"). In the ideal case of a raster infinite in time, this is a convex problem, and therefore there is a unique solution. For the realistic case, the input raster is finite, and several solutions can solve the problem [6]. The algorithm starts from an initial guess of the h_l s and computes the corresponding averages $\mu(m_l)$ using a Monte Carlo method. From this, it computes a variation of the h_l s giving, if possible, a lower Kullback-Leibler divergence (see [40] for details). We proceed this way until no improvement in the Kullback-Leibler divergence is observed any more. At this point, modifying some parameters (see next paragraph) can nevertheless still improve the minimization.

Let us now describe how to compute Gibbs distributions with PRANAS. There are many (an exponential number) a priori possible potentials. In PRANAS we propose four predefined potentials although the user can also define his own one. The options are the following. Here we characterize the potential by the list of monomials \mathcal{M} which compose it.

- **Bernoulli model:** It takes into account individual neurons activity where all neurons

are independent. The potential reads $\phi(\omega) = \sum_{l=1}^N h_l \omega_l(0)$ where N is the number of neurons. Hence, monomials are of type “neuron i is firing at time t ” (Example: $\mathcal{M} = \{\omega_1(0), \omega_2(0), \omega_3(0)\}$ for 3 neurons). This model has range 1 .

- **Ising model:** This paradigmatic model from statistical physics has been used in neuroscience in several papers such as [53, 54, 63, 64]. The corresponding potential has been introduced above. The monomials are of type “neuron i is firing at time t ” and “neuron i and neuron j are simultaneously firing at time t ”. Thus events are instantaneous, and this model does not involve memory and causality (consecutive times are independent under μ , the Gibbs distribution). This model has range 1 (Example for 3 neurons: $\mathcal{M} = \{\omega_1(0), \omega_2(0), \omega_3(0), \omega_1(0)\omega_2(0), \omega_1(0)\omega_3(0), \omega_2(0)\omega_3(0)\}$).
- **Pairwise + Triplets model:** This model has been introduced by [16, 17]. In addition to Ising terms, there are triplets of interactions (e.g. $\omega_1(0)\omega_2(0)\omega_3(0)$). This model too has range 1.
- **Pairwise model.** This is an extension of Ising model where monomials are of type “neuron i is firing at time t ” (single events) and “neuron i is firing at time t and neuron j is firing at time $t+k$ ”, $0 \leq k \leq D$ (pairwise events). This model integrates memory and causality via time dependent pairwise interactions. (Example with range 2 and 2 neurons: $\mathcal{M} = \{\omega_1(0), \omega_2(0), \omega_1(0)\omega_2(0), \omega_1(0)\omega_1(1), \omega_2(0)\omega_2(1), \omega_1(0)\omega_2(1), \omega_1(1)\omega_2(0)\}$).
- **User.** Here the user defines his own potential (Example $\mathcal{M} = \{\omega_1(0), \omega_2(0), \omega_3(0), \omega_1(0)\omega_2(1)\omega_3(2), \dots\}$).

Example 2 How to calculate the Gibbs distribution of a spike train?

1. **FP** `Data>Spikes>Open`
2. **PP** Browse and select the file of spikes.
3. **RP** (Optional) In the sub-panel showing the list of neurons, select a subset of neurons and click on **Keep selected**.
4. **FP** `Analysis>Population analysis`.
5. **PP** Define the **Potential**, either from a file or by setting the type (e.g., **pairwise**) and the range⁴ (e.g., $R=3$). Set the **Maximal pattern length**. For example, if you select 2, the program will seek *in the data* all spike events occurring within 2 successive time steps, and compare the probability of these events, predicted by the model, to the empirical probabilities. In **Simulation**, choose what you want to compute. Possible choices are:
 - (i) **Potential:** Fits the coefficients of the potential.
 - (ii) **Kullback-Leibler divergence:** an estimation of Kullback-Leibler divergence derived from the entropy estimation in [58] and the classical relations between K-L divergence, μ average of ϕ and entropy [6].
 - (iii) **Pattern probabilities:** The confidence plot.
6. **FP** `Analysis>Population analysis>Parametric potential`

⁴The product $N \times R$ somewhat defines the complexity of the model. The larger $N \times R$ the longer the simulation and the memory load. We have been able to run up to $N = 100$, $R = 2$ in reasonable times. Note however that the statistical estimation of a so-huge number of neurons raises the classical problems (*not inherent to our method*) of statistical estimation on a sample, which, e.g. for the retina rarely exceeds a few millions of spikes.

7. **PP** Choose **Initial coefficients**: possible choices are **Current** (in the case when you have made a run before and you want to keep h_{ls}) or 0. For the first run you can choose both as the initial parameters are anyway set to 0 (this corresponds to start from a Bernoulli models where spikes are independent with probability of occurrence $\frac{1}{2}$). Set parameters of the Monte Carlo method to speed up the process (see text for the role of each parameter).
8. **FP** **Population analysis**
9. **RP** **Compute** to do the estimation. The red bar at the bottom indicates that computation is in progress.

Note that in PRANAS the user can fine-tune the probability estimation and speed up the computation in the first steps of the Monte Carlo method by acting on the following parameters (in **FP** **Analysis>Population analysis>Parametric potential**):

- **Convergence bound**: The lower bound of error you require. Simulations stops when the code reaches this value.
- **Tolerance Coefficient**: Allows to filter monomials to compute h_{ls} . For example, if the event m_l appears only, say 3 times in the raster you may consider that it is not significant and must be eliminated from the potential (1). In this case you set **Tolerance Coefficient** to 3.
- **Raster length**: The length of the Monte Carlo raster used to compute the average of monomials for the current values of h_{ls} . This number must increase as you get closer to the solution (typically when you do not get any improvement in the error).
- **Spike flips coefficients**: This defines the number of flips per neuron and per iteration in Monte Carlo methods [40].
- **Delta**: If the distance between predicted and empirical distribution is smaller than **Delta** the Monte Carlo raster is not recomputed. Instead, the average value of monomials is computed via linear response [40]. The number must be decreased as you get closer to the solution (typically when you do not get any improvement in the error).
- **Number of parallel iterations**: We use two kinds of updating, based upon [14]: parallel or sequential. Parallel update sets all h_{ls} in one step. **Number of parallel iterations** tells how many parallel updating of h_{ls} are done before the program stops (and e.g. plots the confidence plot, when selected).
- **Number of sequential iterations**: Sequential update. It computes only one h_l at each step. It is better to use it at the end of the computation, to fine-tune coefficients.

Figure 3 shows different visualizations of the results. In (a), we show a graphical view of the potential's coefficients. In (b), we show the literal form of the potential $\phi(\omega)$. In this example, it is

$$\begin{aligned} \phi(\omega) = & -0.860273 w_1(2) - 0.715493 w_2(2) + \dots - 0.280176 w_0(2)w_2(2) \\ & + \dots - 0.120281 w_0(2)w_3(2)w_5(3) + \dots, \end{aligned} \quad (2)$$

where, e.g., $w_0(2)w_2(2)$ corresponds to the event "neuron zero and neuron two are firing at time two whereas -0.280176 is the corresponding coefficient h_l of this term in the potential. In (c), we show a plot of monomials average value, with empirical average on the abscissa and theoretical

average (predicted by μ) on the ordinate. In (d), we show the evolution of the Hellinger⁵ distance between the model predictions and empirical data, versus the number of iterations. Hellinger distance is natural here as it relies directly on the estimation of the average value of monomials. It provides a quantitative measure of the goodness of fit. Finally, in (e) we show a *confidence plot*. This figure consists of plotting, in log scale, on the abscissa the empirical probability of observed spike blocks and on the ordinate the expected probability of those blocks for the model μ . If the matching were perfect one would have all points aligning on the diagonal. This perfect matching is only possible, however, if the input spike train were infinite. For finite spike trains fluctuations about the exact probability are observed, ruled by Central Limit Theorem. Namely, fluctuations are Gaussian with a variance σ_l , depending on the monomial l and proportional to $\frac{1}{\sqrt{T}}$, T being the raster length (number of time bins). Around the diagonal are drawn error bounds corresponding to $3\sigma_l$, where σ is an estimated empirically. These bounds define a confidence region: if the Gibbs distribution is a perfect estimation of the input raster then points in the confidence plot are distributed inside the confidence region with a probability of 99.7% of the expected averages. The confidence plot provides a qualitative measure of the goodness of the fit.

Reducing the computation time has been a primary concern for us during the development phase. In fact, the most time-consuming routine of PRANAS is for inferring the Gibbs Potential. To face this problem, we introduced a new algorithm based on Monte Carlo sampling [42]. For a large number of neurons, the Monte Carlo-based algorithm offers better computation time than the algorithm proposed in [67]. With a cluster of 64 cores of 2.4GHz speed, PRANAS needs the following amount of time to compute a target distribution (1 iteration): 5 min. for 20 neurons with a pairwise model $R = 2$, 10 minutes for 40 neurons with an Ising model. To infer the Gibbs Distribution, one needs 100-200 iterations on the h_l estimation. For more details on the scalability of this method see [42].

3.2.3 Receptive fields estimation

Beyond tools to analyse spike trains at the single cell and population levels, PRANAS provides specific instruments in the case when spike trains come from evoked activity of neurons from the retina. The user can upload MEA characteristics, the sequences of images of the stimulus and the time stamps. Given this information, PRANAS provides a method to estimate the neuron's receptive fields. The method available in version 1.0.0 is Spike Triggered Average (STA) [8]. The STA can be computed for a single neuron, a subset of neurons or the entire population. Example 3 describes the general procedure.

Example 3 How to estimate receptive fields with STA method?⁶

1. FP Data>Spikes>Open
2. PP Browse and select the file of spikes. Note that the user can select a subset of neurons as in Example 1.
3. FP Data>Multi-Electrode Array>Settings
4. PP Define the MEA configuration, so that, if neurons have a position relative to the array, the spike activity can be displayed at the correct location.

⁵The Hellinger distance between the empirical probability π and the Gibbs probability μ is $d(\pi, \mu) = \frac{1}{\sqrt{2}} \sqrt{\sum_{l=1}^L \left(\sqrt{\pi(m_l)} - \sqrt{\mu(m_l)} \right)^2}$.

⁶To test this example, one can use sample data available on PRANAS website: recording called mouse-P39_17_06_14 (We are indebted to Evelyne Sernagor and Gerrit Hilgen, Newcastle University, who provided us these data and authorized us to use them as a basis for examples.)

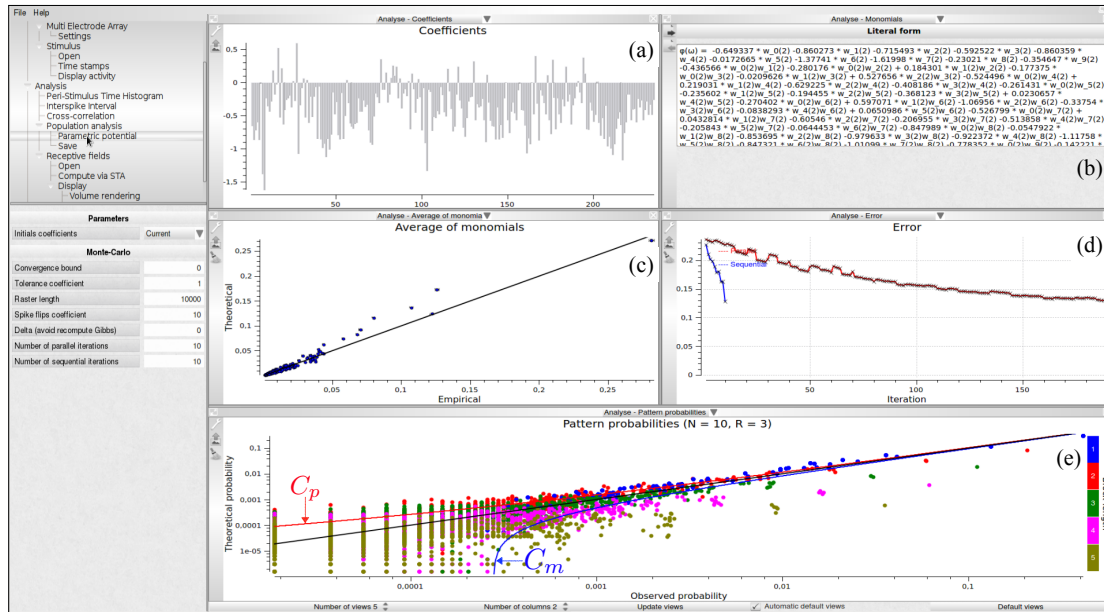


Figure 3: Population analysis view with $N = 10, R = 2$. (a) Graphic view of the potential's coefficients values; the abscissa corresponds to an index associated to a prescribed order on monomials: the N first coefficients corresponds to single events (hence are related to firing rate); by clicking on the histogram bar one makes appear the coefficient value and the corresponding monomial. Ordinate give the value of the coefficient attached to the corresponding monomial. (b) Literal form of the potential. (c) Theoretical average value of monomials versus their empirical average value. To which extents the model predicts the empirical data is drawn with this representation. This allows checking that constraints on empirical averages are respected by the model. (d) Decay of estimation errors versus the number of iterations allowing us to graphically check the convergence of the estimation algorithm (red curve). In the figure several successive runs have been performed. The blue curve shows the evolution of error after each of these trials. (e) Confidence plot. C_p, C_m corresponds respectively to the upper and lower 3σ bound associated with Central Limit Theorem (see text).

5. **[RP]** **Stimulus view** shows the activity of individual neurons w.r.t. MEA array. The user may choose a region of interest to select a subset of neurons. Note that if you have a TEXT file for spikes, no position is available, and we chose to arrange neurons following their order, by rows and columns.
6. **[FP]** **Data>Stimulus>Open**
7. **[PP]** Browse to choose the directory containing the sequence of white noise images. Note that all images should be in this directory and ordered by name. All standard formats are accepted (e.g., PNG, JPG, TIFF).
8. **[FP]** **Data>Stimulus>Time stamps**: Time stamps of the exact offset of each image during the experiment.
9. **[PP]** Browse and select the file. Time stamps can be imported from a .txt (row n contains the starting time of image n) or HDF5 [70].
10. **[FP]** **Analysis>Receptive fields>Compute via STA**

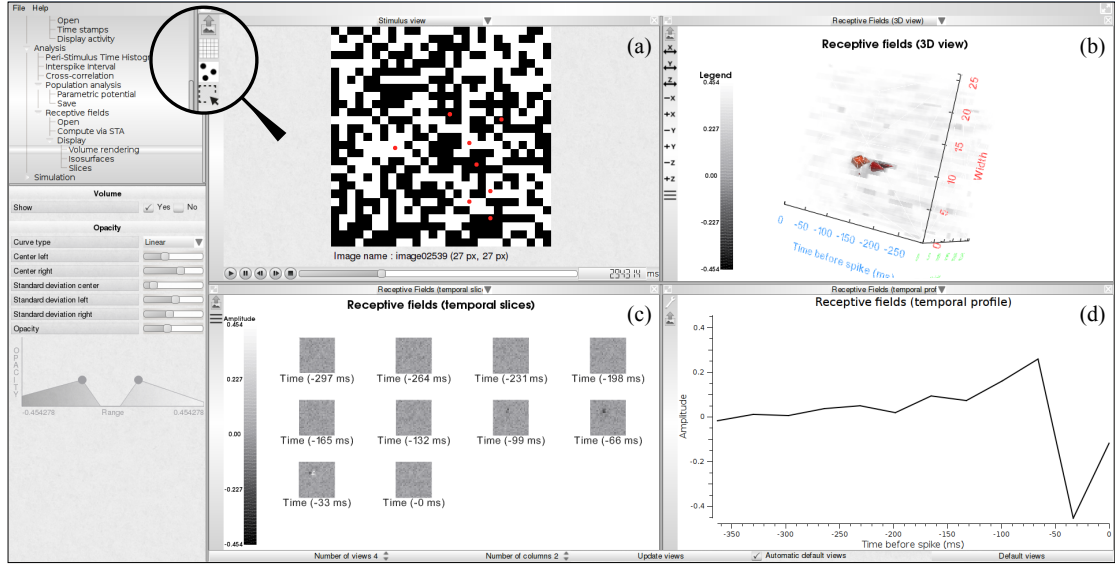


Figure 4: Receptive field estimation using the STA approach. (a) White noise image sequence with spiking activity superimposed as red dots. (b) 3D volume visualization of the receptive field of one neuron. (c) Temporal slices of the receptive field ($RF(\cdot, \cdot, z)$). Slices are in increasing time order from top to bottom and left to right. Time period between two slices is 33ms. (d) Temporal profile passing through the peak activity location of the spatio-temporal volume ($RF(x_M, y_M, \cdot)$ where $(x_M, y_M, z_M) = \operatorname{argmax}_{x,y,z} RF(x, y, z)$).

11. **RP** **Output directory:** Choose the directory where the receptive fields will be saved, as a sequence of PNG files and in HDF5 format. Choose the number of images to be averaged before each spike with **Time depth (number of slices)**. Then click on **Compute**.
12. **FP** **Analysis>Receptive fields>Display** allows four types of visualization.
13. **RP** The user can display the receptive field of interest by selecting the neuron in **Receptive Fields** subpanel and **Update views**.

A receptive field is stored in a regular grid in a three-dimensional space. Each voxel in that grid, denoted by $RF(x, y, z)$, stores the value of the receptive field at each spatial position ($x \times s_d, y \times s_d$) and temporal depth $z \times t_d$, where s_d and t_d denote respectively the spatial and temporal resolutions. The temporal resolution is estimated from the time stamps file as the average difference between two successive time stamps. The number of time slices of the receptive field, n_f , is a user-defined parameter. The first spatial slice ($x, y, z = 0$) corresponds to the average spike triggered stimuli at time $-(n_f - 1)t_d$ before the spike, the second slice ($x, y, z = 1$) corresponds to the average spike triggered stimuli at time $-(n_f - 2) \times t_d$ before the spikes and so on. In PRANAS we propose several displays of that volume (2D and 3D), as illustrated in Fig. 4.

The time spent on the estimation of receptive fields depends on the parameters. For example, on a computer equipped with a Intel Core i7@2.8GHz and 32 GB of memory it takes about two minutes to estimate the receptive fields of 4000 neurons with $64 \times 64 \times 12$ voxels each.

3.3 Simulation of spike trains

3.3.1 Simulation of spike trains from statistics

PRANAS gives the possibility to generate spike trains from Gibbs distributions. This can be useful if, for example, one wants to generate spike trains with prescribed spatio-temporal correlations so as to test a statistical method of analysis. There are two different ways:

1. **[FP]** `Simulation>ComputeSpikes>GibbsRaster>current`: if distribution comes from a population analysis (see Sec. 3.2.2).
2. **[FP]** `Simulation>ComputeSpikes>GibbsRaster>File`: if distribution has been defined by the user and stored in a file containing the Gibbs potential form.

A Gibbs probability distribution (defined by Gibbs potential of the form (1)) is naturally associated with a Markov chain, with memory $D = R - 1$, whose transition probabilities can be computed from the potential ϕ [68, 6, 10]. The invariant distribution μ of this chain is the Gibbs distribution associated to ϕ . Therefore, given a potential of the form (1) it is easy to generate a sample raster distributed according to μ using Monte Carlo method [42]. PRANAS affords this functionality allowing to generate rasters with spatio-temporal correlations tuned by the parameters h_l in ϕ .

3.3.2 Simulation of spike trains from a retina simulator

Another strength of PRANAS is to provide a way to generate spike trains that mimic retina's outputs. To do so, PRANAS has integrated and extended the VIRTUAL RETINA simulator [69] formerly developed in our team.⁷

In a nutshell, VIRTUAL RETINA is a software to perform large-scale simulations of biologically-plausible retinas. Given a retina configuration which can be fully customized and an input video as visual stimulus, VIRTUAL RETINA simulates the spiking output for different cell types. VIRTUAL RETINA has been shown to reproduce a broad range of experimental data at single cell level, from salamander, cat and primate retinas, and has been used in several theoretical studies [36, 37, 39, 1, 11, 12, 66]. The underlying model includes a non-separable spatio-temporal linear model of filtering in the Outer Plexiform Layer, a shunting feedback at the level of bipolar cells, and a spike generation process using a network generalization of the noisy leaky integrate-and-fire neurons to model Ganglion Cells (GCells). Note that VIRTUAL RETINA was designed to be used via a command line (there was no GUI available).

By integrating VIRTUAL RETINA software into PRANAS platform, we allowed this simulation software to be used through a GUI. We also extended VIRTUAL RETINA with the aim to reproduce statistically coherent responses at a population level. Indeed, outputs of the initial VIRTUAL RETINA version were successfully compared to experimental data at single cell level but could not reproduce collective statistics at a population level. This is because GCells in the early version were not connected. They were modelled by independent leaky-integrate and fire neurons receiving their input from bipolar cells, but with no lateral connectivity (due to amacrine cells - ACells - in the retina). As a consequence correlations in GCells spikes were only due to statistics of the stimulus and overlapping receptive fields.

In the new version of the retina simulator embedded in PRANAS, GCells are connected laterally so as to explore the effects of connectivity on retinal responses to stimuli. More precisely, the IPL is now composed of discrete time leaky-integrate and fire neurons introduced in [55] and

⁷VIRTUAL RETINA website: <http://virtualretina.inria.fr>. VIRTUAL RETINA is under Inria CeCILL-C license, IDDN.FR.001.210034.000.S.P.2007.000.31235.

studied mathematically in [4, 5]. We have chosen this model because of its simplicity, fast response, and the fact that its collective dynamics are well known. In a nutshell, the model comes from the time discretization of the leaky-integrate and fire model whose sub-threshold dynamics reads:

$$C \frac{dV}{dt} = -g_L(V - V_L) + I(t) + \sigma_B B(t), \quad (3)$$

for $V < \theta$, where θ is the firing threshold. Here C is the membrane capacity, g_L the leak conductance, V_L is the leak reversal potential, $B(t)$ is a Gaussian noise (mean zero and variance 1) and σ_B controls the amplitude of this noise. Finally, $I(t)$ is an external current. In our case, this is the bipolar current coming from the OPL (see [69] for details).

Let $\tau_L = \frac{C}{g_L}$ be the leak characteristic time. We consider now a time discretization with a time step dt (here it is fixed, $dt = 1\text{ms}$) and we set $\gamma = \left(1 - \frac{dt}{\tau_L}\right)$. Note that dt has to be quite smaller than τ_L to have a reasonable description of the biophysics. Therefore $\gamma \in [0, 1[$. Then, the full dynamics (below and above threshold) of the membrane potential V_i of neuron i is given by:

$$V_i(t+1) = \gamma V_i(t)(1 - Z_i) + \frac{I_i(t)}{C} + \frac{\sigma_B}{C} B(t),$$

where Z is the binary spike label:

$$Z_i = \begin{cases} 1, & \text{if } V_i \geq \theta; \\ 0, & \text{otherwise.} \end{cases}$$

Thus Z_i is 1 whenever neuron i spikes. Here $1 - Z_i$ models the reset. In this equation, neurons are not coupled. We add then a connectivity through synaptic weights W_{ij} where neuron j (pre synaptic) acts on neuron i (post synaptic) upon spiking. We have now:

$$V_i(t+1) = \gamma V_i(t)(1 - Z_i) + \frac{I_i(t)}{C} + \frac{1}{C} \sum_{j=1}^N W_{ij} Z_j + \frac{\sigma_B}{C} B(t). \quad (4)$$

For a complete description see [4, 5]. Clearly, this modelling of lateral connectivity, although usual in the field of neural networks models, is rough when compared to the real lateral connectivity in the IPL involving amacrine cells having a complex dynamics. Elaborating more realistic coupling is under current investigations.

The simulator allows to tune the parameters leak ($\gamma \in [0, 1]$); neuronal noise ($\sigma_B > 0$); membrane capacity (C); threshold (θ) and the connectivity matrix (W). The connectivity between neurons is set through the connectivity matrix. One can simulate independent neurons by choosing **none** or connected neurons using **sparse** or **dense** schemes. One can also upload a predefined connectivity matrix offering the possibility to explore its impact on spike statistics. For example, we provide on the website an example of ACells-like connectivity pattern.

Example 4 shows how to generate spikes using PRANAS and Fig. 5 illustrates an example of simulation. Note that user can find online retina configuration files and videos sequences to test the simulator.

Example 4 Running the retina simulator.⁸

1. FP Data>Stimulus>Open

⁸To run this example one can use data available on PRANAS website, for example the **martin-walk** image sequence and the **cat_X_cell_DLIF.xml** retina configuration file which corresponds to the result shown in Fig. 5.

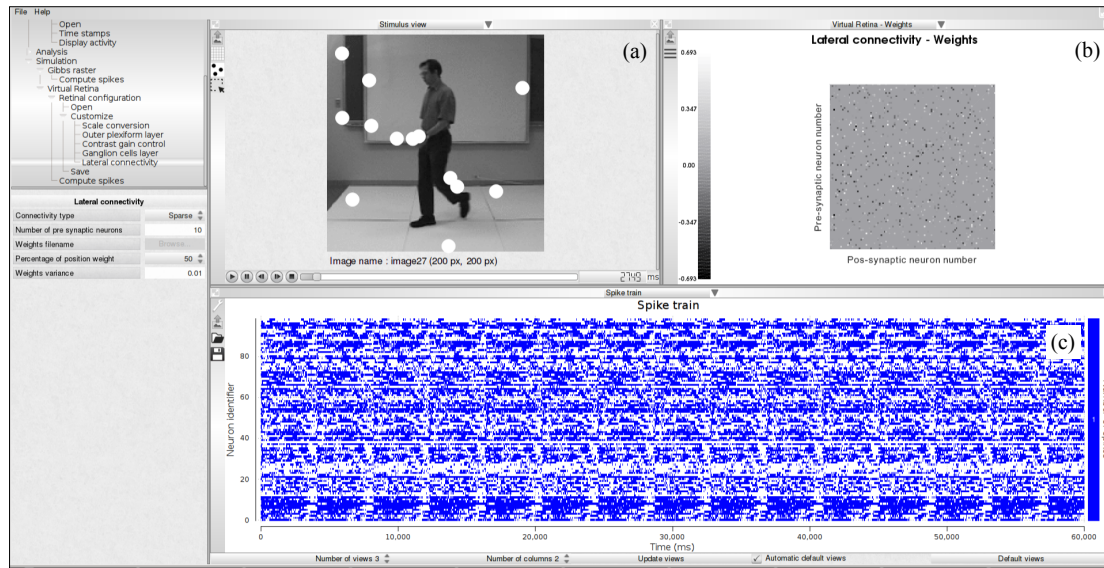


Figure 5: Spike generation from our retina simulator. (a) Input image sequence with spiking activity super-imposed (white blobs). (b) Connectivity matrix chosen for the simulation, here random. (c) Simulated spike train.

2. **PP** Browse to choose the directory containing the sequence.
3. **RP** **Stimulus sequences** subpanel: The sequence of images is loaded with a default display duration of 100ms per image (**Display time** column). This value can be manually set or defined from time stamps file (see Example 3).
4. **FP** **Simulation>Virtual Retina>Retinal configuration>Open**⁹
5. **PP** Browse and select the XML files containing the parameters of the retina.
6. **FP** **Simulation>Virtual Retina>Retinal configuration>Customize**: Once loaded, the user can still change parameters of the retina.
7. **FP** **Simulation>Virtual Retina>Compute spike**.
8. **PP** **Compute** to get the spikes.

The time spent in the generation of spikes with the retina simulator depends on the parameters. For example it takes about six minutes to generate the spikes corresponding to Fig. 5 on a laptop equipped with a Intel Core i7-6820HK CPU@2.70GHz. This was obtained with the image sequence **martin-walk** (200×200 pixels, 41 frames) and the **cat_X_cell_DLIF.xml** retina configuration file (100 neurons, sparse connectivity with 1000 connections out of 10000 possible connections).

⁹Note that steps 4–6 can be skipped and one can directly generate spikes in step 7 using a proposed default configuration.

4 Conclusion

In this paper we have introduced PRANAS, a new free¹⁰ platform for retinal analysis and simulation. PRANAS provides a retina simulator allowing to transform any video into spike trains, together with sophisticated methods to analyse spike trains, coming from simulations but also experiments. As explained, PRANAS (version 1.0.0) includes a range of original methods from the state-of-the-art [6, 69] which are now available to the neuroscience community. More precisely, PRANAS intends to be useful for the neuroscience community in a large sense, i.e., not only experienced computational neuroscientists. To do so, we decided to make all methods implemented therein accessible through a friendly GUI. No scripting is needed to run analysis and simulation methods. This represents a major advantage to promote interdisciplinary neuroscience and we believe that PRANAS helps in this direction.

However, we are certainly aware that this advantage could also be seen as a limitation of the software. Indeed, inability to script analyses could be a limitation that can make systematic analysis of large datasets tedious and error prone. It makes also difficult to link the functionalities of this toolbox to more extensive data analysis workflow. For those reasons, we also offer some functionalities that run on the command line. A non-exhaustive list of tools that can be used from the command line is **SimulateRetina** (simulate retinal response), **Correlations** (compute the average cross-correlations of a given raster), **SpikeTriggerAverage** (compute the average spike triggered stimuli).¹¹ We expect to have the platform fully available with scripting in a forthcoming version.

In this first release of PRANAS, we have focused on the following aspects:

- The user experience: We optimized the ergonomics of interactions between the user and the interface. No scripting is needed to analyse or generate the spike trains.
- The richness of toolboxes: We developed a variety of methods ranging from classical tools to population analysis, including a method for receptive fields estimation. In addition, we provide two simulators, one inspired in the retina, the other from rasters statistics analysis.
- The computational performance: We parallelized a selection of functions to make possible to handle faster large populations of neurons¹².

By putting together functions related to retina simulation and analysis, PRANAS intends to be an original platform that will encourage joint modeling and experimental studies. The synergy between these two areas of functionality will be in particular useful to define better retina simulators by confronting simulated output w.r.t. real cell recordings. A typical use case is to start from a real cell recording of a retina, to analyse its receptive field structure, and use that information to define the XML retina configuration file so to define a virtual retina having similar characteristics as the real one. Another use case that we target is to start again from a real cell recording of a retina, analyse spike train statistics and compare them with the ones given by the simulator. Such a comparison is very informative and will suggest improvements of the retina simulator to increase its biological plausibility.

¹⁰PRANAS is under Inria CeCILL-C license, IDDN.FR.001.190004.000.S.P.2014.000.31235. Binaries can be freely downloaded.

¹¹These commands can be found in the directory `pranas/bin`. Help of each tool is given with the command line: `toolName -h`.

¹²Parallelization concerns every loop in our C++ code where iterations can be computed independently. To do so, we used OpenMP so that PRANAS parallel processes can run on a personal computer equipped with multi-core processors. More precisely, four functions were parallelized: (i) the loading of rasters for all file formats, (ii) the statistical analysis functions to generate potentials, compute divergence and estimate patterns probabilities, (iii) the estimation of receptive fields and (iv) the retina simulator.

Here, we presented its main features, and we refer the interested reader to its website¹³ for downloads and more information (see, e.g., tutorials to get started). We hope that PRANAS becomes a useful tool for neuroscientists to analyse spike trains and we expect to improve it thanks to the users' feedback. Our goal is to progressively enrich PRANAS with the latest research results, to facilitate the transfer of new methods to the community. Future work will focus on improving several existing functions regarding efficiency in time and memory consumptions. We will include methods for population analysis in the non-stationary case as well as other statistical analysis models. We are working on better methods for receptive fields estimation [13]. We are also developing extensions of the retina simulator model so that it could serve as a satisfactory model at a population level. Finally, as a general objective, we also plan to improve the computational power of PRANAS in order to handle even larger networks.

Funding

This work was supported by KEOPS ANR-CONICYT, the EC IP project FP7-ICT-2011-9 no. 600847 (RENVISION) and FP7-IDEAS-ERC no. 227747 (NERVI), the French ministry of Research and University of Nice (EDSTIC), INRIA ADT and by the ECOS-Sud program (grant C13E06).

Acknowledgements

We warmly acknowledge Michael J. Berry, Maria-Jose Escobar, Matthias Hennig, Ruben Herzog, Gerrit Hilgen, Evgenia Kartsaki, Gaia Lombardi, Olivier Marre, Thierry Mora, Adrian Palacios, Cesar Ravello, Horacio Rostro, Vivien Robinet, Selma Souihel, Evelyne Sernagor, Gasper Tkacik, Juan-Carlos Vasquez for their help in designing PRANAS. The authors also thank the reviewers for their constructive criticisms and valuable comments which helped us improve the manuscript.

References

- [1] G. Basalyga, M. A. Montemurro, and T. Wennekers. Information coding in a laminar computational model of cat primary visual cortex. *J. Comput. Neurosci.*, 34:273–83, 2013.
- [2] A. Benoit, A. Caplier, B. Durette, and J. Herault. Using human visual system modeling for bio-inspired low level image processing. *Computer Vision and Image Understanding*, 114(7):758–773, 2010.
- [3] M. Carandini, J. B. Demb, V. Mante, D. J. Tollhurst, Y. Dan, B. A. Olshausen, J. L. Gallant, and N. C. Rust. Do we know what the early visual system does? *Journal of Neuroscience*, 25(46):10577–10597, Nov. 2005.
- [4] B. Cessac. A discrete time neural network model with spiking neurons. rigorous results on the spontaneous dynamics. *J. Math. Biol.*, 56:311–345, 2008.
- [5] B. Cessac. A discrete time neural network model with spiking neurons II. dynamics with noise. *J. Math. Biol.*, 62:863–900, 2011.

¹³PRANAS website: <http://pranas.inria.fr>

- [6] B. Cessac and A. Palacios. Spike train statistics from empirical facts to theory: the case of the retina. In F. Cazals and P. Kornprobst, editors, Modeling in Computational Biology and Biomedicine: A Multidisciplinary Endeavor, Lectures Notes in Mathematical and Computational Biology (LNMCB), pages 261–302. Springer-Verlag, Berlin, Heidelberg, 2012.
- [7] B. Cessac, H. Rostro-Gonzalez, J.-C. Vasquez, and T. Viéville. How gibbs distribution may naturally arise from synaptic adaptation mechanisms: a model based argumentation. J. Stat. Phys., 136(3):565–602, August 2009.
- [8] E. J. Chichilnisky. A simple white noise analysis of neuronal light responses. Network (Bristol, England), 12:199–213, 2001.
- [9] R. Cofré and B. Cessac. Dynamics and spike trains statistics in conductance-based integrate-and-fire neural networks with chemical and electric synapses. Chaos, Solitons & Fractals, 2013.
- [10] R. Cofre and B. Cessac. Exact computation of the maximum-entropy potential of spiking neural-network models. Phys. Rev. E, 89(052117), 2014.
- [11] E. Doutsis, L. Fillatre, M. Antonini, and J. Gaulmin. Retinal-inspired filtering for dynamic image coding. In IEEE International Conference on Image Processing (ICIP), pages 3505–3509, Quebec city, Canada, 2015.
- [12] E. Doutsis, L. Fillatre, M. Antonini, and J. Gaulmin. Video analysis and synthesis based on a retinal-inspired frame. In 23rd European Signal Processing Conference (EUSIPCO), pages 2226–2230, Nice, France, 2015. IEEE.
- [13] A. Drogoul, G. Aubert, B. Cessac, and P. Kornprobst. A new nonconvex variational approach for sensory neurons receptive field estimation. In 6th International Workshop on New Computational Methods for Inverse Problems (NCMIP), Cachan, France, 2016.
- [14] M. Dudík, S. J. Phillips, and R. E. Schapire. Performance Guarantees for Regularized Maximum Entropy Density Estimation, page 472–486. Springer Berlin Heidelberg, Berlin, Heidelberg, 2004.
- [15] E. Ferrea, A. Maccione, L. Medrihan, T. Nieuw, D. Ghezzi, P. Baldelli, F. Benfenati, and L. Berdondini. Large-scale, high-resolution electrophysiological imaging of field potentials in brain slices with microelectronic multielectrode arrays. Front. Neural Circuits, 6(November):80, 2012.
- [16] E. Ganmor, R. Segev, and E. Schneidman. The architecture of functional interaction networks in the retina. The journal of neuroscience, 31(8):3044–3054, 2011.
- [17] E. Ganmor, R. Segev, and E. Schneidman. Sparse low-order interaction network underlies a highly correlated and learnable neural population code. PNAS, 108(23):9679–9684, 2011.
- [18] S. Garcia and N. Fourcaud-Trocmé. Openelectrophy: an electrophysiological data-and analysis-sharing framework. Frontiers in neuroinformatics, 3, 2009.
- [19] K. S. Ginsburg, J. A. Johnsen, and L. Michael W. Common noise in the firing of neighbouring ganglion cells in goldfish retina. J. Physiol., 351:433–450, 1984.
- [20] D. H. Goldberg, J. D. Victor, E. P. Gardner, and D. Gardner. Spike train analysis toolkit: enabling wider application of information-theoretic techniques to neurophysiology. Neuroinformatics, 7(3):165–178, 2009.

- [21] T. Gollisch and M. Meister. Eye smarter than scientists believed: neural computations in circuits of the retina. *Neuron*, 65(2):150–164, Jan. 2010.
- [22] M. Greschner, J. Shlens, C. Bakolitsa, G. D. Field, J. L. Gauthier, L. H. Jepson, A. Sher, A. M. Litke, and E. J. Chichilnisky. Correlated firing among major ganglion cell types in primate retina. *J. Physiol.*, 589(Pt 1):75–86, Jan. 2011.
- [23] J. Hérault. *Vision: Images, Signals and Neural Networks Models of Neural Processing in Visual Perception*. World Scientific Publishing Co., Inc., River Edge, NJ, USA, 2010.
- [24] R. Herzog, J. Araya, M. Pizarro, B. Cessac, C. Ravello, M.-J. Escobar, and A. Palacios. From Habitat to Retina: Neural Population Coding using Natural Movies. Bernstein Conference, Sept. 2015.
- [25] R. Herzog, M. J. Escobar, B. Cessac, and A. Palacios. Dimensionality reduction on maximum entropy models on spiking networks. *Plos. Comp. Bio.* (submitted), 2017.
- [26] C. Hillar and F. Effenberger. Robust discovery of temporal structure in multi-neuron recordings using hopfield networks. *Procedia Computer Science*, 53(L50):365–374, 2015.
- [27] R. A. Ince, A. Mazzoni, R. S. Petersen, and S. Panzeri. Open source tools for the information theoretic analysis of neural data. *Frontiers in neuroscience*, 4, 2010.
- [28] E. Jaynes. Information theory and statistical mechanics. *Phys. Rev.*, 106:620, 1957.
- [29] J. S. Kim, M. J. Greene, A. Zlateski, K. Lee, M. Richardson, S. C. Turaga, M. Purcaro, M. Balkam, A. Robinson, B. F. Behabadi, M. Campos, W. Denk, H. S. Seung, and Eye-Wirers. Space-time wiring specificity supports direction selectivity in the retina. *Nature*, 509(331-336), 2014.
- [30] M. Lidiérth. sigtool: a matlab-based environment for sharing laboratory-developed software to analyze biological signals. *Journal of neuroscience methods*, 178(1):188–196, 2009.
- [31] H. Lorach, R. Benosman, O. Marre, S.-H. Ieng, J. A. Sahel, and S. Picaud. Artificial retina: the multichannel processing of the mammalian retina achieved with a neuromorphic asynchronous light acquisition device. *Journal of Neural Engineering*, 9(6):066004, Oct. 2012.
- [32] O. Marre, S. El Boustani, Y. Frégnac, and A. Destexhe. Prediction of spatiotemporal patterns of neural activity from pairwise correlations. *Physical review letters*, 102(13):138101–138105, Apr. 2009.
- [33] A. Martinez-Alvarez, A. Olmedo-Payá, S. Cuenca-Asensi, J. M. Ferrandez, and E. Fernandez. RetinaStudio: A bioinspired framework to encode visual information. *Neurocomputing*, 114:45–53, Aug. 2013.
- [34] R. H. Masland. Cell populations of the retina: The proctor lecture. *Investigative Ophthalmology and Visual Science*, 52(7):4581–4591, June 2011.
- [35] R. H. Masland. The Neuronal Organization of the Retina. *Neuron*, 76(2):266–280, Oct. 2012.
- [36] K. Masmoudi, M. Antonini, and P. Kornprobst. Another look at the retina as an image scalar quantizer. In *Proceedings of the International Symposium on Circuits and Systems (ISCAS)*, pages 3076–3079, Paris, France, 2010.

- [37] T. Masquelier. Relative spike time coding and stdp-based orientation selectivity in the early visual system in natural continuous and saccadic vision: a computational model. Journal of Computational Neuroscience, 32(3):425–441, 2012.
- [38] R. Meier, U. Egert, A. Aertsen, and M. P. Nawrot. {FIND}: A unified framework for neural data analysis. Neural Networks, 21(8):1085 – 1093, 2008. Neuroinformatics Neuroinformatics.
- [39] A. Mohemmed, G. Lu, and N. Kasabov. Evaluating SPAN Incremental Learning for Hand-written Digit Recognition. In International Conference on Neural Information Processing, pages 670–677, Doha, Qatar, 2012. Springer Berlin Heidelberg.
- [40] H. Nasser and B. Cessac. Parameters estimation for spatio-temporal maximum entropy distributions: application to neural spike trains. Entropy, 16(4):2244–2277, 2014.
- [41] H. Nasser, S. Kraria, and B. Cessac. Enas: a new software for neural population analysis in large scale spiking networks. In Twenty Second Annual Computational Neuroscience Meeting, page 57, Paris, France, July 2013. Organization for Computational Neurosciences.
- [42] H. Nasser, O. Marre, and B. Cessac. Spatio-temporal spike train analysis for large scale networks using the maximum entropy principle and montecarlo method. Journal of Statistical Mechanics: Theory and Experiment, 2013(03):P03006, 2013.
- [43] B. Odermatt, A. Nikolaev, and L. Lagnado. Encoding of luminance and contrast by linear and nonlinear synapses in the retina. Neuron, 73(4):758 – 773, 2012.
- [44] F. J. Pelayo, S. Romero, C. A. Morillas, A. Martinez, E. Ros, and E. Fernandez. Translating image sequences into spike patterns for cortical neuro-stimulation. Neurocomputing, 58–60:885–892, 2004.
- [45] C. Pouzat and A. Chaffiol. Automatic spike train analysis and report generation. an implementation with r, r2html and star. Journal of neuroscience methods, 181(1):119–144, 2009.
- [46] R. Pröpper and K. Obermayer. Spyke viewer: a flexible and extensible platform for electrophysiological data analysis. Frontiers in neuroinformatics, 7:26, 2013.
- [47] P. Quaglio, A. Yegenoglu, E. Torre, D. M. Endres, and S. Gruen. Detection and evaluation of spatio-temporal spike patterns in massively parallel spike train data with spade. Frontiers in Computational Neuroscience, 11:41, 2017.
- [48] C. Ravello, R. Herzog, B. Cessac, M.-J. Escobar, and A. Palacios. Spectral dimension reduction on parametric models for spike train statistics. 12e Colloque de la Société des Neurosciences , May 2015. Poster.
- [49] F. Rieke, D. Warland, R. de Ruyter van Steveninck, and W. Bialek. Spikes, Exploring the Neural Code. The M.I.T. Press, Cambridge, Massachusetts, USA, 1996.
- [50] Y. Roudi and J. Hertz. Mean field theory for non-equilibrium network reconstruction. Phys. Rev. Lett., 106(048702), 2011.
- [51] Y. Roudi, S. Nirenberg, and P. Latham. Pairwise maximum entropy models for studying large biological systems: when they can work and when they can’t. PLOS Computational Biology, 5(5), 2009.

- [52] Y. Roudi, J. Tyrcha, and J. A. Hertz. Ising model for neural data: Model quality and approximate methods for extracting functional connectivity. *Physical Review E*, page 051915, 2009.
- [53] E. Schneidman, M. Berry, R. Segev, and W. Bialek. Weak pairwise correlations imply strongly correlated network states in a neural population. *Nature*, 440(7087):1007–1012, 2006.
- [54] J. Shlens, G. Field, J. Gauthier, M. Grivich, D. Petrusca, A. Sher, A. Litke, and E. Chichilnisky. The structure of multi-neuron firing patterns in primate retina. *Journal of Neuroscience*, 26(32):8254, 2006.
- [55] H. Soula, G. Beslon, and O. Mazet. Spontaneous dynamics of asymmetric random recurrent spiking neural networks. *Neural Computation*, 18(1), 2006.
- [56] M. Spacek, T. Blanche, and N. Swindale. Python for large-scale electrophysiology. *Frontiers in neuroinformatics*, 2, 2008.
- [57] I. H. Stevenson and K. P. Kording. How advances in neural recording affect data analysis. *Nature Neuroscience*, 14(2):139–142, Jan. 2011.
- [58] S. Strong, R. Koberle, R. de Ruyter van Steveninck, and W. Bialek. Entropy and information in neural spike trains. *Phys. Rev. Lett*, 80(1):197–200, 1998.
- [59] K. Takahashi, S. Kim, T. Coleman, K. Brown, A. Suminski, M. Best, and N. Hatsopoulos. Large-scale spatiotemporal spike patterning consistent with wave propagation in motor cortex. *Nature Communications*, 6:7169, 2015.
- [60] A. Tang, D. Jackson, J. Hobbs, W. Chen, J. L. Smith, H. Patel, A. Prieto, D. Petrusca, M. I. Grivich, A. Sher, P. Hottowy, W. Dabrowski, A. M. Litke, and J. M. Beggs. A maximum entropy model applied to spatial and temporal correlations from cortical networks *In Vitro*. *The Journal of Neuroscience*, 28(2):505–518, January 2008.
- [61] G. Tkačik, O. Marre, T. Mora, D. Amodei, M. B. 2nd, and W. Bialek. The simplest maximum entropy model for collective behavior in a neural network. *J. Stat. Mech.*, 2013, March 2013.
- [62] G. Tkačik, J. S. Prentice, V. Balasubramanian, and E. Schneidman. Optimal population coding by noisy spiking neurons. *PNAS*, 107(32):14419–14424, August 2010.
- [63] G. Tkačik, E. Schneidman, M. Berry II, and W. Bialek. Ising models for networks of real neurons. *arXiv q-bio/0611072*, 2006.
- [64] G. Tkačik, E. Schneidman, M. J. Berry II, and W. Bialek. Spin glass models for a network of real neurons. *arXiv preprint arXiv:0912.5409*, 2009.
- [65] E. Torre, P. Quaglio, M. Denker, T. Brochier, A. Riehle, and S. Grun. Synchronous spike patterns in macaque motor cortex during an instructed-delay reach-to-grasp task. *Journal of Neuroscience*, 36:8329–8340, 2016.
- [66] P. Vance, S. A. Coleman, D. Kerr, G. Das, and T. McGinnity. Modelling of a retinal ganglion cell with simple spiking models. In *IEEE International Joint Conference Neural Networks*, pages 1–8, Killarney, Ireland, 2015.

- [67] J.-C. Vasquez, B. Cessac, and T. Viéville. Entropy-based parametric estimation of spike train statistics. In *Statistical Mechanics of Learning and Inference*, Mariehamn, Finland, May 2010.
- [68] J. C. Vasquez, O. Marre, A. G. Palacios, M. J. Berry, and B. Cessac. Gibbs distribution analysis of temporal correlation structure on multicell spike trains from retina ganglion cells. *J. Physiol. Paris*, 106(3–4):120–127, May 2012.
- [69] A. Wohrer and P. Kornprobst. Virtual retina: a biological retina model and simulator, with contrast gain control. *Journal of Computational Neuroscience*, 26(2):219–249, 2009.
- [70] S. Zordan, M. Zanotto, T. Niels, S. Di Marco, H. Amin, A. Maccione, and L. Berdondini. A scalable high performance client/server framework to manage and analyze high dimensional datasets recorded by 4096 CMOS-MEAs. In *7th International IEEE/EMBS Conference on Neural Engineering (NER)*, Montpellier, France, 2015.

Contents

1	Introduction	3
2	General presentation	4
3	PRANAS main functions	6
3.1	Data	6
3.2	Analysis	7
3.2.1	Classical analysis	7
3.2.2	Population analysis	7
3.2.3	Receptive fields estimation	12
3.3	Simulation of spike trains	15
3.3.1	Simulation of spike trains from statistics	15
3.3.2	Simulation of spike trains from a retina simulator	15
4	Conclusion	18



**RESEARCH CENTRE
SOPHIA ANTIPOLIS – MÉDITERRANÉE**

2004 route des Lucioles - BP 93
06902 Sophia Antipolis Cedex

Publisher
Inria
Domaine de Voluceau - Rocquencourt
BP 105 - 78153 Le Chesnay Cedex
inria.fr

ISSN 0249-6399